LIGO-T050228-00-R

Population statistics of gravitational-wave pulsars

Milivoje Lukic
Mentors: Teviet Creighton and Réjean Dupuis

September 22, 2005

Abstract

Gravitational waves emitted by spinning neutron stars provide a direct probe of their internal structure and mass distribution. Searches for gravitational waves from pulsars using LIGO data have already set upper limits on GW emission from several individual pulsars. We use those observations to study the distribution of quadrupole moments of the galactic pulsar population. A Bayesian methodology is developed to use aggregate data from all observed pulsars to determine properties of the population, such as the average and maximum quadrupole moment. We estimate the sensitivity of the method on simulated noise for varying signal-to-noise ratios and number of pulsars in our sample. We also predict the sensitivity of Advanced LIGO to these population parameters using the current set of known pulsars. The method is applied to results for individual pulsars obtained from the LIGO S2 science run.

1 Introduction

1.1 Gravitational waves emitted by spinning neutron stars

The General Theory of Relativity predicts the existence of gravitational waves. According to GR, gravitational waves are generated when masses are accelerated. The amplitude of the generated gravitational waves is

$$h_{\mu\nu} = \frac{2G}{c^4 r}\frac{d^2 Q_{\mu\nu}}{dt^2} \tag{1}$$

where Q denotes the reduced quadrupole moment

$$Q_{\mu\nu} = \int \rho(\vec{r})(x_\mu x_\nu - \frac{1}{3}\delta_{\mu\nu} r^2) dV. \tag{2}$$

Among the possible sources of gravitational waves are spinning neutron stars. A spinning neutron star is expected to emit gravitational waves if it is not perfectly symmetric about its rotation axis. Some mechanisms have been suggested that could make neutron star asymmetric. These mechanisms include strains in a solid crust left over from its formation [1] and large internal magnetic fields [2]. For the purposes of modelling of emitted gravitational waves, neutron stars are often modelled as triaxially shaped rigid bodies rotating around one of their principal axes [3]. The ellipticity of such a neutron star is defined as

$$\epsilon = (I_2 - I_1)/I_3 \tag{3}$$

where I_1, I_2, I_3 denote the principal moments of inertia (and I_3 corresponds to the axis of rotation). From the above formulae, it follows that the gravitational wave amplitude of such a neutron star is

$$h \approx \frac{16\pi^2 G f^2}{c^4 r} I_3 \epsilon \tag{4}$$

where f denotes the frequency of rotation of the pulsar. The frequency of the emitted waves is twice the frequency of rotation, $f_{\mathrm{GW}} = 2f$.

The maximum sustainable ellipticity of a conventional neutron star is of the order of 10^{-7}, leading to gravitational wave amplitude of the order of $10^{-24} \times (f/1000\mathrm{Hz})^2 \times (r/1\mathrm{kpc})^{-1}$. However, there are other models of structure of compact stars, which allow ellipticities up to the order of 10^{-4} [4].

1.2 Bayesian analysis

The Bayesian approach to probability theory differs from the classical approach in the definition of probability. While the classical (frequentist) approach defines probability as the relative frequency of an event, the Bayesian approach defines probability as the degree of belief. The Bayesian definition of probability allows probabilities to be assigned to hypotheses. This allows the use of Bayes' theorem

$$p(\text{Hypothesis}|\text{Data}) \propto p(\text{Hypothesis})p(\text{Data}|\text{Hypothesis}). \tag{5}$$

Here $p(\text{Hypothesis})$ is the prior probability of the hypothesis, which is based on the background information, $p(\text{Data}|\text{Hypothesis})$ is the likelihood of the data given the hypothesis and the background information, and $p(\text{Hypothesis}|\text{Data})$ is the posterior probability of the hypothesis, based on the background information and the data.

The often disputed part of Bayesian analyses is the choice of priors. While the prior $p(\text{Hypothesis})$ is sometimes chosen as one that will best reflect all our prior knowledge, sometimes it is more desirable to choose a flat prior that will allow us to focus on new information we get from the experimental data [5]. Priors are often chosen with help of the maximum entropy principle, which states that given a set of constraints which the prior must satisfy, we should choose the prior with the maximum value of the entropy, defined as

$$H = -\int p(x) \ln p(x) dx. \tag{6}$$

Bayesian analysis is often used for parameter estimation, where the hypothesis consists of conjectured values for one or more parameters, taking values from the parameter space. Once we have the result of the analysis in the form of a posterior $p(x|\text{Data})$, there is the question of interpreting this result. One relevant result is the single most probable value, defined as the value $x_{\max}$ of the parameter where the posterior reaches its maximal value $p(x_{\max}|\text{Data}) = \max p$. However, if presented by itself, this value contains no information about the expected error level. One way to express that error level is the full width of the half-maximum, defined as the length of the interval $(x_{\text{l}}, x_{\text{r}})$ such that

$$p(x_{\text{l}}|\text{Data}) = p(x_{\text{r}}|\text{Data}) = \frac{1}{2} p(x_{\max}|\text{Data}). \tag{7}$$

Another way to express the result are confidence intervals. Since the obtained posteriors are usually not normalized, we normalize them to satisfy

$$\int p(x|\text{Data}) dx = 1. \tag{8}$$

For a confidence level p (typically chosen as 68%, 95% or 99%), the confidence interval is defined as the minimum-width interval $(x_{\text{l,p}}, x_{\text{r,p}})$ such that

$$\int_{x_{\text{l,p}}}^{x_{\text{r,p}}} p(x|\text{Data}) dx = p. \tag{9}$$

In other words, we claim that the parameter x is, with the probability p, constrained within the limits $(x_{\text{l,p}}, x_{\text{r,p}})$.

1.3 Objectives

The goal of this project is to determine from experimental data the probability distributions of the maximum and mean ellipticity of the galactic pulsar population, which we denote by $\epsilon_{\max}$ and $\bar{\epsilon}$, respectively. Gravitational-wave measurements give information about the amplitude h_0 of gravitational waves. Methods have been developed to determine probability distribution functions $p(h_{0i}|P_i)$, where P_i denotes data for pulsar i [6]. We intend to combine the probability distributions of gravitational wave amplitudes that were determined for several pulsars individually.

From eq. (4) we see that h_0, apart from being dependent on the frequency and distance of the pulsar (which are well determined for all pulsars to be included in our analysis), is proportional to the product of two factors, I_3 and ϵ. While the value of I_3 is often approximated by the canonical value $10^{38}\,\mathrm{kg\,m^2}$, we choose to postpone using the approximation for I_3 and to perform all computations with the quadrupole moment $Q = I_3\epsilon$ instead of ϵ. $Q_{\max}$ and $\bar{Q}$ will denote the maximum and mean quadrupole moment of the population.

The input data used are the posterior probability distributions $p(h_0|P_i)$. Eq. (4) gives the linear scaling of all probability distributions containing h_0 as a parameter to Q probability distributions. The posteriors were obtained using flat priors, thus for the corresponding likelihoods it holds $p(h_0|P_i) \propto p(P_i|h_0)$. Scaling $p(P_i|h_0)$ linearly by the factor $\frac{16\pi^2 G f^2}{c^4 r}$, we reach the probability distributions $p(P_i|Q_i)$ on which we will base further discussion.

2 Method

2.1 Likelihoods $p(\{P_i\}|Q_{\max})$ and $p(\{P_i\}|\bar{Q})$

For a given value of $Q_{\max}$,

$$p(\{P_i\}|Q_{\max}) = \prod_i p(P_i|Q_{\max}), \tag{10}$$

the product ranging over all pulsars included in the analysis. Further,

$$p(P_i|Q_{\max}) = \int_0^{+\infty} p(P_i|Q_i)p(Q_i|Q_{\max})dQ_i. \tag{11}$$

Combining eqs. (10) and (11), we find

$$p(\{P_i\}|Q_{\max}) = \prod_i \int_0^{+\infty} p(P_i|Q_i)p(Q_i|Q_{\max})dQ_i. \tag{12}$$

In an analogous manner, we derive

$$p(\{P_i\}|\bar{Q}) = \prod_i p(P_i|\bar{Q}), \tag{13}$$

$$p(P_i|\bar{Q}) = \int_0^{+\infty} p(P_i|Q_i)p(Q_i|\bar{Q})dQ_i, \tag{14}$$

$$p(\{P_i\}|\bar{Q}) = \prod_i \int_0^{+\infty} p(P_i|Q_i)p(Q_i|\bar{Q})dQ_i. \tag{15}$$

Apart from the input data $p(P_i|Q_i)$, the above formulae require the probability distributions $p(Q_i|Q_{\max})$ and $p(Q_i|\bar{Q})$. These priors are determined according to the principles outlined in section 1.2.

2.2 The prior $p(Q_i|Q_{\max})$

In this case the only information we have about the quadrupole moments is that they are constrained to the interval $[0, Q_{\max}]$. Therefore, we use the least informative prior

$$p(Q_i|Q_{\max}) = \begin{cases} \dfrac{1}{Q_{\max}} & \text{, for } 0 \le Q_i \le Q_{\max} \\ 0 & \text{, otherwise.} \end{cases} \tag{16}$$

2.3 The prior $p(Q_i|\bar{Q})$

In this case quadrupole moments are constrained only by $Q_i \geq 0$, but the prior is constrained by the conditions

$$\int_0^{+\infty} p(Q_i|\bar{Q})dQ_i = 1 \tag{17}$$

and

$$\int_0^{+\infty} p(Q_i|\bar{Q})Q_i dQ_i = \bar{Q}. \tag{18}$$

Solving the maximum entropy principle gives the form of the prior

$$p(Q_i|\bar{Q}) = \mathrm{e}^{AQ_i+B}. \tag{19}$$

Combining eq. (19) with eq. (17) gives $\mathrm{e}^B = -A$, and combining it with eq. (18) gives $A = -1/\bar{Q}$. Thus,

$$p(Q_i|\bar{Q}) = \frac{1}{\bar{Q}}\mathrm{e}^{-Q_i/\bar{Q}}. \tag{20}$$

2.4 Priors $p(Q_{\max})$, $p(\bar{Q})$ and posteriors $p(Q_{\max}|\{P_i\})$, $p(\bar{Q}|\{P_i\})$

Following the principles outlined in section 1.2, we choose flat priors $p(Q_{\max})$ and $p(\bar{Q})$. Now eq. (5) gives

$$p(Q_{\max}|\{P_i\}) \propto p(\{P_i\}|Q_{\max}) = \prod_i \int_0^{+\infty} p(P_i|Q_i)p(Q_i|Q_{\max})dQ_i \tag{21}$$

and

$$p(\bar{Q}|\{P_i\}) \propto p(\{P_i\}|\bar{Q}) = \prod_i \int_0^{+\infty} p(P_i|Q_i)p(Q_i|\bar{Q})dQ_i. \tag{22}$$

3 Normalization of results

In order to be able to extract confidence intervals from the posteriors $p(Q_{\max}|\{P_i\})$ and $p(\bar{Q}|\{P_i\})$, they must be normalized. Since we allow $Q_{\max}$ and $\bar{Q}$ to range over all non-negative values, we must analyze the convergence of the integrals $\int_0^{+\infty} p(Q_{\max}|\{P_i\})dQ_{\max}$ and $\int_0^{+\infty} p(\bar{Q}|\{P_i\})d\bar{Q}$. Since $p(Q_{\max}|\{P_i\})$ and $p(\bar{Q}|\{P_i\})$ are continuous functions, taking a finite value at 0, divergence can only occur at $+\infty$. For $Q_{\max}$, observe that

$$\begin{aligned} p(Q_{\max}|\{P_i\}) \propto p(\{P_i\}|Q_{\max}) &= \prod_{i=1}^{N} \frac{1}{Q_{\max}} \int_0^{Q_{\max}} p(P_i|Q_i)dQ_i & (23)\\ &= \frac{1}{{Q_{\max}}^N} \prod_{i=1}^{N} \int_0^{Q_{\max}} p(P_i|Q_i)dQ_i & (24)\\ &\sim \frac{1}{{Q_{\max}}^N}, \quad \text{when } Q_{\max} \to \infty. & (25) \end{aligned}$$

Since $\int_1^{+\infty} {Q_{\max}}^{-N} dQ_{\max}$ is divergent for $N = 1$ and convergent for $N > 1$, the posterior $p(Q_{\max}|\{P_i\})$ is normalizable when $N > 1$.

For $\bar{Q}$, observe that

$$p(\bar{Q}|P_i) \propto \frac{1}{\bar{Q}} \int_0^{+\infty} \mathrm{e}^{-Q_i/\bar{Q}} p(P_i|Q_i)dQ_i. \tag{26}$$

Since

$$\lim_{\bar{Q}\to+\infty} \mathrm{e}^{-Q_i/\bar{Q}} = 1 \tag{27}$$

holds for every Q_i,

$$\lim_{\bar{Q}\to\infty} p(\bar{Q}|P_i) \propto \frac{1}{\bar{Q}} \int_0^{+\infty} p(P_i|Q_i)dQ_i = \frac{1}{\bar{Q}}. \tag{28}$$

Thus, $p(\bar{Q}|\{P_i\}) \sim 1/\bar{Q}^N$ as $\bar{Q} \to \infty$, and as for $Q_{\max}$, the posterior is normalizable for $N > 1$.

Thus, this method of analysis can only be used when there is data for more than one pulsar available.

4 Method testing

We are interested in the output that this method will produce for various kinds of input data. The results should depend on the number of pulsars included in the analysis, as well as the sensitivity to different pulsars. We will begin by studying two extreme cases: the case of signals without noise and the case of noise without signals. After that we will proceed to the general case of various signal-to-noise ratios. Throughout this section, we will work with simulated data, and we will use lowercase q to denote the simulated values of the parameters in question, i.e. q_i will be the quadrupole moment of pulsar i, and $\bar{q}$, $q_{\max}$ will denote the mean and maximum quadrupole moment of the pulsars included in our analysis. N will denote the number of pulsars included in the analysis.

4.1 The case of signals without noise

An ideal signal for the pulsar i would be a likelihood $p(P_i|Q_i) = \delta(Q_i - q_i)$. Thus, let us consider having likelihoods for N pulsars that are δ-functions peaked at $q_1, q_2, \ldots, q_n$. Substituting into eqs. (11), (12), (13), (15),

$$p(P_i|Q_{\max}) = p(q_i|Q_{\max}) = \begin{cases} 0 & \text{for} \quad Q_{\max} < q_i \\ \dfrac{1}{Q_{\max}} & \text{for} \quad Q_{\max} \geq q_i \end{cases} \tag{29}$$

$$p(Q_{\max}|\{P_i\}) \propto p(\{P_i\}|Q_{\max}) = \begin{cases} 0 & \text{for} \quad Q_{\max} < q_{\max} \\ \frac{1}{{Q_{\max}}^N} & \text{for} \quad Q_{\max} \geq q_{\max} \end{cases} \tag{30}$$

$$p(P_i|\bar{Q}) = p(q_i|\bar{Q}) = \frac{1}{\bar{Q}} \mathrm{e}^{-q_i/\bar{Q}} \tag{31}$$

$$p(\bar{Q}|\{P_i\}) \propto p(\{P_i\}|\bar{Q}) = \frac{1}{\bar{Q}^N} \mathrm{e}^{-N\bar{q}/\bar{Q}} \tag{32}$$

It is worth noting that the derived posteriors for $Q_{\max}$ and $\bar{Q}$ do not depend on the individual q_i, but only on $q_{\max}$ and $\bar{q}$, respectively.

From eqs. (30) and (32) it is straightforward to verify that the posteriors for $Q_{\max}$ and $\bar{Q}$ peak at $q_{\max}$ and $\bar{q}$, respectively. The importance of that fact lies in the behaviour of the posteriors when $N \to \infty$: the lower and upper confidence limits then tend to the peak values, and the posteriors $p(Q_{\max}|\{P_i\})$ and $p(\bar{Q}|\{P_i\})$ tend to $\delta(Q_{\max} - q_{\max})$ and $\delta(\bar{Q} - \bar{q})$. The lower and upper confidence limits, as a function of N, are shown in Figure 1.

4.2 The case of noise without signals

Another question of interest is the upper limits one can set on the population when no gravitational waves are detected from any of the individual pulsars. Let us assume that we have input data for N pulsars without a detectable signal and with noise of the same level. The input likelihoods are modelled as Gaussian distributions with mean value 0 and standard deviation $\sigma = 1$ (changing the standard deviation would introduce only a scaling factor; thus, we use $\sigma = 1$ and express all upper limits in units of σ). For large N, the upper limits decrease asymptotically as $1/\sqrt{N}$. The upper limits, as functions of N, are shown in Figure 2.

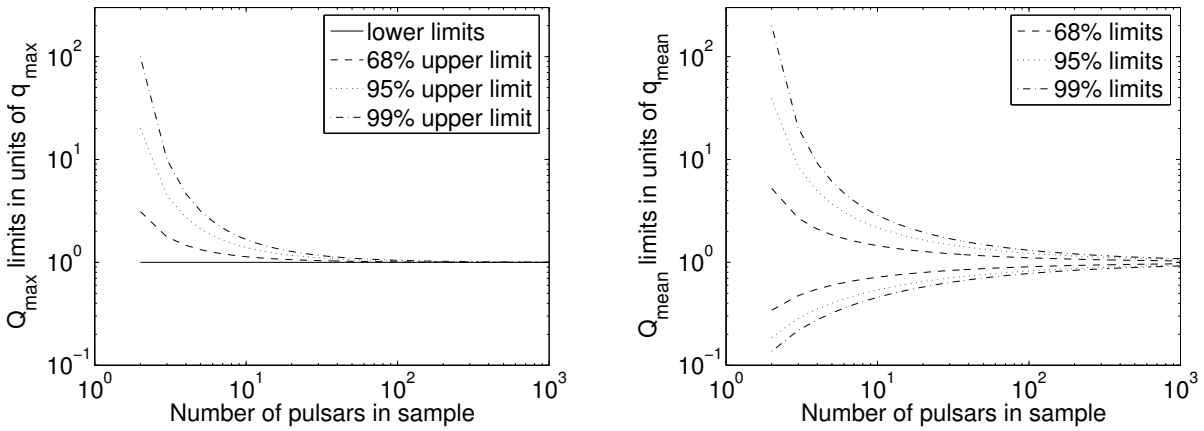

Figure 1: The 0.68, 0.95 and 0.99 upper and lower limits for $Q_{\max}$ and $\bar{Q}$ for varying number of pulsars in the case of ideal signals. Notice that all the lower limits for $Q_{\max}$ are equal to $q_{\max}$

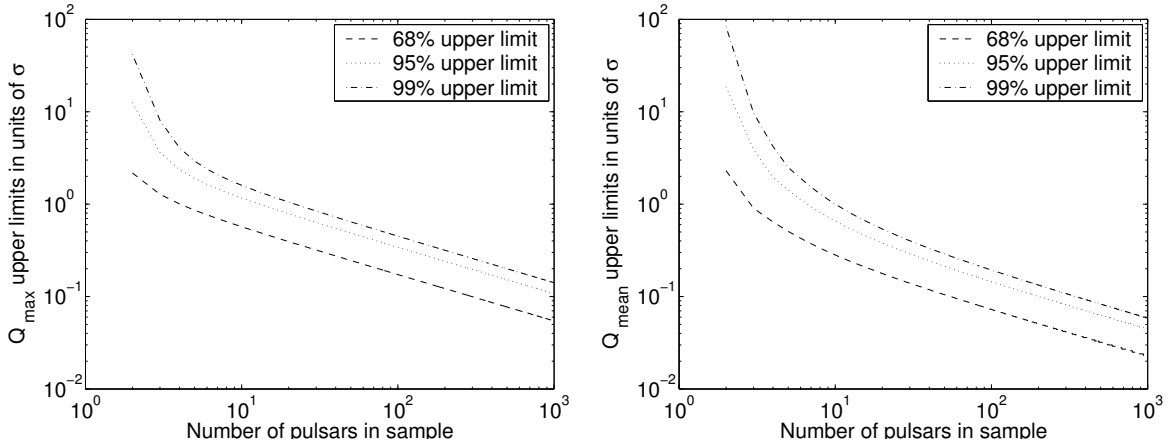

Figure 2: The 0.68, 0.95 and 0.99 upper limits for $Q_{\max}$ and $\bar{Q}$ for varying number of pulsars in the case of input data with no detections. Notice that the upper limits decrease as $1/\sqrt{N}$

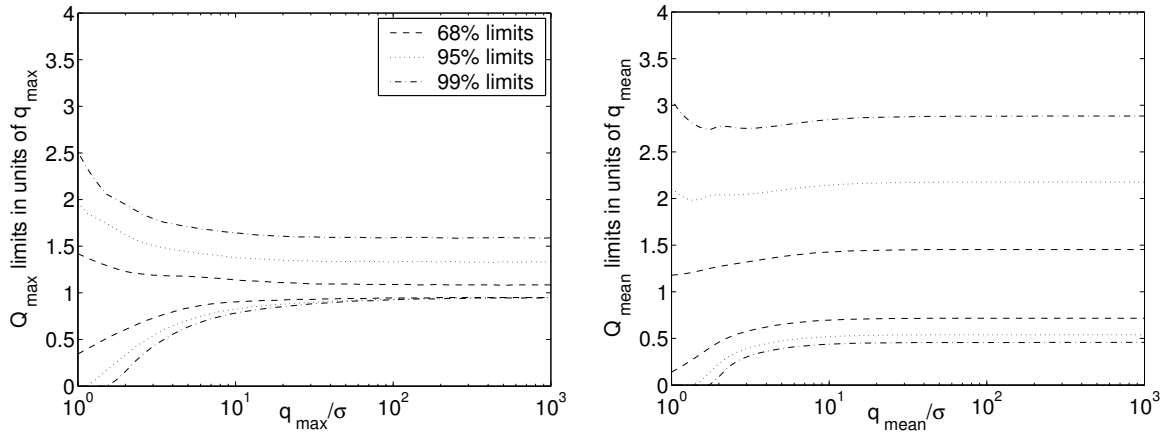

Figure 3: The 0.68, 0.95 and 0.99 limits for varying signal-to-noise ratio for a sample size of 10 pulsars

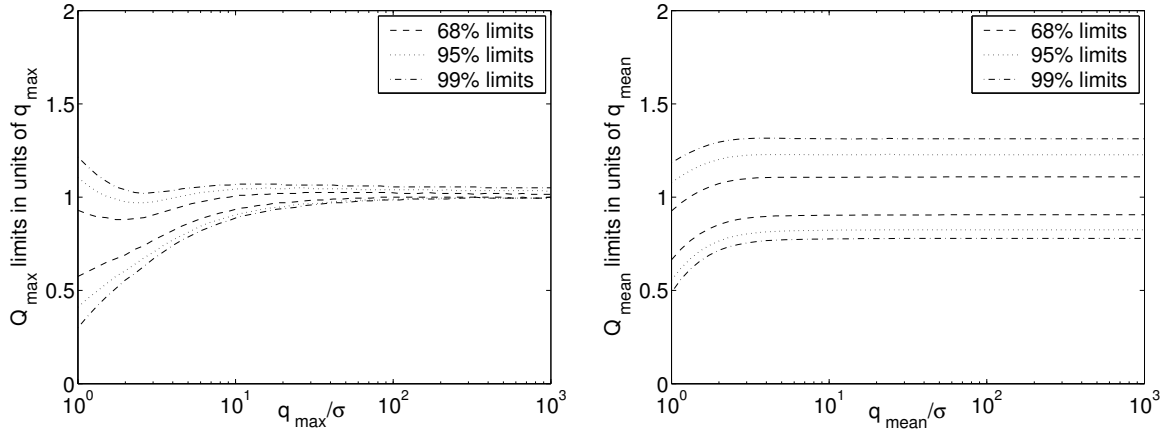

Figure 4: The 0.68, 0.95 and 0.99 limits for varying signal-to-noise ratio for a sample size of 100 pulsars

4.3 Results for varying signal-to-noise ratio

Another question of interest is the output of the method when it is applied to data which contains detections as well as a noise level. To investigate that case, we simulate the likelihoods $p(Q_i|P_i)$ as Gaussian distributions with mean value q_i and standard deviation σ. We vary σ and observe the resulting upper and lower limits as functions of $q_{\max}/\sigma$ or $\bar{q}/\sigma$, which can be regarded as measures of the precision. We perform this analysis for $N = 10$ and $N = 100$. The results are given in Figures 3 and 4.

5 Analysis of S2 data

Throughout this section we will adopt the convention $I_3 = 10^{38}\,\mathrm{kg\,m^2}$ and present our results in terms of $\epsilon_{\max}$ and $\bar{\epsilon}$.

We used the results from [6] where S2 data has been searched for signals from 28 pulsars, with the tightest individual 95% upper limit $\epsilon < 4.8 \times 10^{-6}$ for pulsar J2124-3358. The rotational frequencies and distances of the pulsars included in the analysis have been taken from [7]. From the results of those searches we obtain

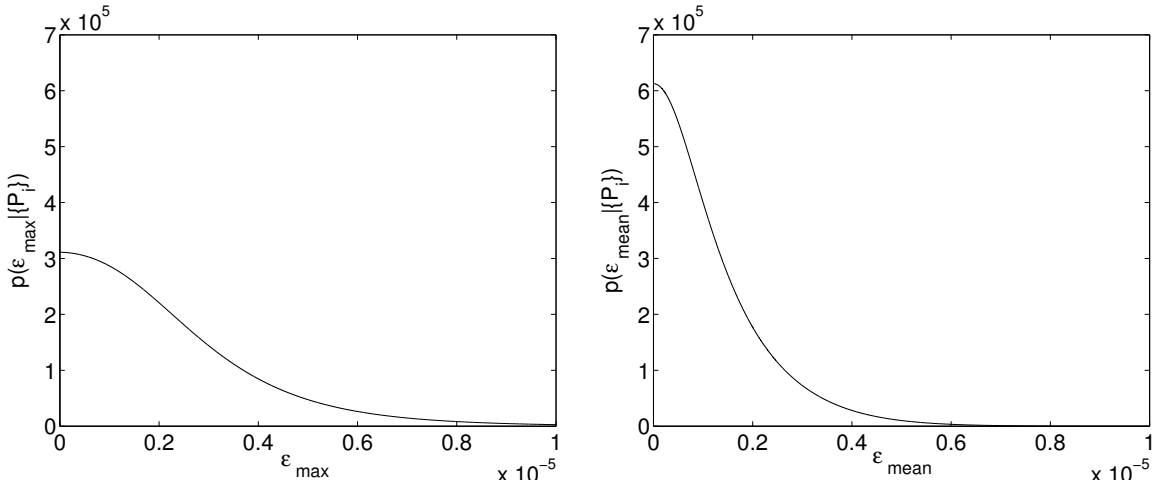

Figure 5: The posteriors $p(\epsilon_{\max}|\{P_i\})$ and $p(\bar{\epsilon}|\{P_i\})$ obtained from S2 data

the posteriors $p(\epsilon_{\max}|\{P_i\})$ and $p(\bar{\epsilon}|\{P_i\})$, shown in Figure 5. The resulting upper limits are

$$\epsilon_{\max,95\%} = 5.9 \times 10^{-6}, \tag{33}$$

$$\bar{\epsilon}_{95\%} = 3.4 \times 10^{-6}. \tag{34}$$

Likelihoods $p(P_i|Q_i)$ have different widths for different pulsars. It can be expected that our results $p(Q_{\max}|\{P_i\})$ and $p(\bar{Q}|\{P_i\})$ will be dominated by a few of the most precise individual likelihoods, while data from the remaining pulsars will not give a substantial improvement, due to their distance from Earth. Pulsars included in the S2 data analysis have been arranged in order of increasing 95% upper limits. For N varying between 2 and 28, the analysis has been performed for only the N pulsars with the least 95% upper limits. The resulting upper limits for $\epsilon_{\max}$ and $\bar{\epsilon}$ are retrieved and presented in Figure 6 as functions of N. This confirms that, after the ~ 10 "best" pulsars have been analyzed, there is little to be gained by including the remaining pulsars.

6 Expected sensitivity of Advanced LIGO

In this section we study the expected performance of our technique to data with the predicted sensitivity of Advanced LIGO. We assume that no detection is made by such a detector, simulate the likelihoods $p(Q_i|P_i)$ and analyze the results obtained with those likelihoods.

Following [6], the 95% upper limit set on an individual pulsar's GW emission is

$$h_{95} = 15.3\sqrt{\frac{S_n(f_{\rm GW})}{T}} \tag{35}$$

where $S_n(f)$ is the sensitivity of the detector to signals of frequency f, $f_{\rm GW} = 2f_{\rm rot}$ is the frequency of the emitted gravitational waves, and T is the observation time in seconds. Likelihoods for individual pulsars are modelled as Gaussian distributions centered at 0. For such distributions the 95% upper limit is 2σ, where σ is the variance of the distribution. Combining with eq. (4),

$$\sigma = 7.7\frac{c^4 r\sqrt{S_n(2f)}}{16\pi^2 G f^2\sqrt{T}} \tag{36}$$

Thus, if the noise curve $S_n(f)$ and the frequencies and distances of the pulsars are known, the likelihoods $p(Q_i|\{P_i\})$ can be simulated. There are 230 currently known pulsars with $f_{\rm rot} > 5\,$Hz (i.e. with gravitational

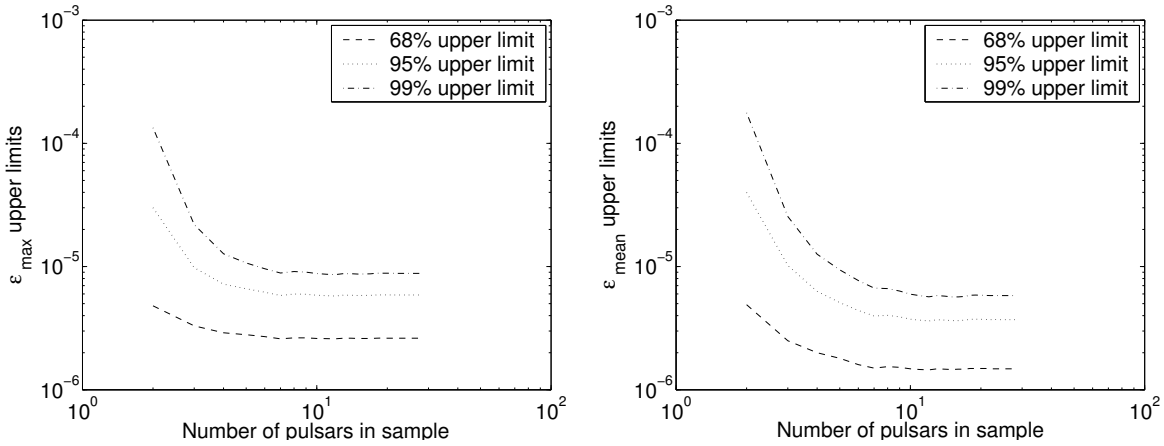

Figure 6: The 95% upper limits of posteriors $p(\epsilon_{\rm max}|\{P_i\})$ and $p(\bar{\epsilon}|\{P_i\})$ obtained from S2 data by using only data from the N pulsars with the tightest individual upper limits on ϵ_i

wave emission in the Advanced LIGO frequency band) and with known distances from the Solar System [7]. For Advanced LIGO sensitivity at 1 year of observations, with simulated data for those 230 pulsars, the upper limits set on $\epsilon_{\rm max}$ and $\bar{\epsilon}$ are

$$\epsilon_{\rm max,95\%} = 1.0 \times 10^{-8}, \tag{37}$$

$$\bar{\epsilon}_{95\%} = 5.3 \times 10^{-9}. \tag{38}$$

For comparison, note that the tightest 95% upper limit set on an individual pulsar by data simulated in this way is $\epsilon < 4.5 \times 10^{-9}$ for pulsar J0437-4715. If the method is applied to only the N pulsars with the tightest 95% upper limits, with N ranging from 2 to 230, we get the upper limits for $\epsilon_{\rm max}$ and $\bar{\epsilon}$ as functions of N, shown on Figure 7. Here, again, after the ~ 30 "best" pulsars have been analyzed, there is little to be gained by including the remaining pulsars.

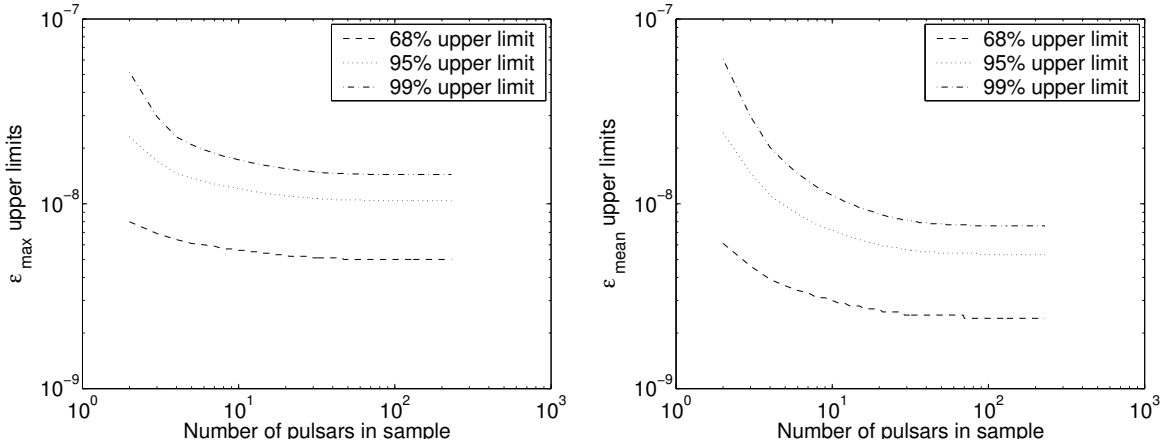

Figure 7: The 95% upper limits of posteriors $p(\epsilon_{\rm max}|\{P_i\})$ and $p(\bar{\epsilon}|\{P_i\})$ obtained from hypothetical data at Advanced LIGO sensitivity by including only the N pulsars with the tightest individual upper limits in ϵ_i

7 Conclusions

In this report we present a method to obtain information about the maximum and mean ellipticity of the galactic pulsar population based on observational data. We study the behaviour of the method for different kinds of data. It is demonstrated how the uncertainty level of the result is dominated by two factors: the precision of the measurements for individual pulsars and the size of the pulsar sample.

We reach the conclusion that there is a $1/\sqrt{N}$ decrease of upper limits in the case of identical pulsars. However, in the galactic pulsar population detections for different pulsars will have quite different sensitivities. We test the dependance on the sample size with S2 data and simulated Advanced LIGO data. There we see that in such a situation, only the most sensitive individual pulsars significantly affect the resulting upper limit.

We apply the method to real data, obtaining upper limits for $\epsilon_{\max}$ and $\bar{\epsilon}$ shown in eqs. (33) and (34). We predict the sensitivity of Advanced LIGO to $\epsilon_{\max}$ and $\bar{\epsilon}$ using the current set of known pulsars, reaching (in the case of no detection made for any of the known pulsars) the values in eqs. (37) and (38). Comparing those results with the tightest upper limits set on the ellipticities of the individual pulsars, note that the $\epsilon_{\max}$ and $\bar{\epsilon}$ upper limits are comparable with the tightest upper limit set on the ellipticity of an individual pulsar.

References

[1] D.I. Jones. Gravitational waves from rotating strained neutron stars. Classical and Quantum Gravity, 19:1255, 2002.

[2] C. Cutler. Gravitational waves from neutron stars with large toroidal B fields. Physical Review D, 66:084025, 2002.

[3] M. Zimmermann and E. Szedenits. Gravitational waves from rotating and precessing rigid bodies - Simple models and applications to pulsars. Physical Review D, 20:351, 1979.

[4] B.J. Owen. Maximum elastic deformations of compact stars with exotic equations of state. astro-ph/0503399, 2005.

[5] D.S. Sivia. Data Analysis: A Bayesian Tutorial. New York: Oxford University Press, 1996.

[6] R.J. Dupuis. Bayesian searches for gravitational waves from pulsars, PhD Thesis, University of Glasgow, 2004.

[7] http://www.atnf.csiro.au/research/pulsar/psrcat/